

# C-terminal ECFP Fusion Impairs Synaptotagmin 1 Function

CROWDING OUT SYNAPTOTAGMIN 1\*

Received for publication, August 2, 2004, and in revised form, November 3, 2004  
Published, JBC Papers in Press, November 23, 2004, DOI 10.1074/jbc.M408757200

Weiping Han<sup>‡§¶</sup>, Jeong-Seop Rhee<sup>||\*\*</sup>, Anton Maximov<sup>‡</sup>, Weichun Lin<sup>‡¶¶</sup>, Robert E. Hammer<sup>§§</sup>,  
Christian Rosenmund<sup>||\*\*</sup>, and Thomas C. Südhof<sup>‡§¶</sup> ¶¶

From the <sup>‡</sup>Center for Basic Neuroscience, the Departments of <sup>§§</sup>Molecular Genetics, <sup>§§</sup>Biochemistry, and <sup>‡¶¶</sup>Cell Biology, and <sup>¶¶</sup>Howard Hughes Medical Institute, the University of Texas Southwestern Medical Center, Dallas, Texas 75390-9111, the <sup>||</sup>Departments of Molecular and Human Genetics and of Neuroscience, Baylor College of Medicine, Houston, Texas 77030, and <sup>\*\*</sup>Max-Planck-Institut für biophysikalische Chemie, 37070 Göttingen, Germany

To allow the monitoring of synaptotagmin 1 trafficking *in vivo*, we generated transgenic mice expressing a synaptotagmin 1-enhanced cyan fluorescent protein (ECFP) fusion protein under control of the Thy1 promoter. Transgenic synaptotagmin 1-ECFP is expressed throughout the brain where it localizes to synapses and marks synapses *in vivo*. However, when we crossed transgenic synaptotagmin 1-ECFP mice with synaptotagmin 1 knock-out mice, we detected no rescue of survival or function. Furthermore, viral overexpression of synaptotagmin 1-ECFP in synaptotagmin 1-deficient neurons failed to restore normal Ca<sup>2+</sup>-triggered release, whereas overexpression of wild type synaptotagmin 1 did so efficiently. To determine whether synaptotagmin 1-ECFP is non-functional because the ECFP-fusion interferes with its biochemical activities, we measured Ca<sup>2+</sup>-independent binding of synaptotagmin 1-ECFP to SNARE complexes, and Ca<sup>2+</sup>-dependent binding of synaptotagmin 1-ECFP to phospholipids and to itself. Although the apparent Ca<sup>2+</sup> affinity of synaptotagmin 1-ECFP was decreased compared with wild type synaptotagmin 1, we observed no major changes in Ca<sup>2+</sup>-dependent or -independent activities, indicating that the non-functionality of the synaptotagmin 1-ECFP fusion protein was not because of inactivation of its biochemical properties. These data suggest that synaptotagmin 1-ECFP is suitable for monitoring synaptic vesicle traffic *in vivo* because the synaptotagmin 1-ECFP marks synaptic vesicles without participating in exocytosis. In addition, the data demonstrate that synaptotagmin 1 function requires a free C terminus, possibly because of spatial constraints at the release sites.

Synapses are the major points of information processing in brain. The number, structure, and properties of synapses change dramatically during the development and maturation of the brain and possibly as a function of experience (see Refs. 1 and 2 for a review of such mechanisms). Visualizing synapses directly would provide a valuable tool for studying synaptogenesis and synaptic plasticity. Recent advances in transgenic techniques have provided exciting methods for examining neuronal shape in living animals (reviewed in Ref. 3). This was

spectacularly achieved with the generation of transgenic mice in which green fluorescent protein (GFP)<sup>1</sup>-derivatives are expressed under control of the Thy1 promoter in a manner that allows the reproducible synthesis of the transgenic protein in only a subset of neurons (4, 5). These mice were invaluable, for example, in examining the stability of synapses in adult brain (6, 7). However, although the selective labeling of a subset of neurons in transgenic mice (4, 5) provides an advantage for longitudinal studies of plastic changes in individual neurons, it is disadvantageous for studies of entire neuronal populations.

A possible strategy for labeling presynaptic terminals in transgenic mice would be to express specifically presynaptic molecules that are labeled with GFP. In pursuing such a strategy, we have examined the localization, properties and function of a chimeric synaptic protein (synaptotagmin 1; Ref. 8) fused to a GFP-derivative (ECFP) (9). Synaptotagmin 1 is an abundant synaptic vesicle protein that contains an N-terminal intraluminal sequence, a single transmembrane region, a central linker, and two C-terminal C<sub>2</sub>-domains. The C<sub>2</sub>-domains account for the majority of the synaptotagmin 1 sequence and function as separate Ca<sup>2+</sup>-binding domains in a complex with phospholipids (10–12). Synaptotagmin 1 functions as a Ca<sup>2+</sup> sensor for the fast component of Ca<sup>2+</sup>-triggered exocytosis in vertebrate neurons (13), neuroendocrine cells (14), and *Drosophila* neurons (15). Changing the apparent Ca<sup>2+</sup> affinity of synaptotagmin 1 causes an equivalent change in the Ca<sup>2+</sup> affinity of release (16, 17), but the precise mechanism of action of synaptotagmin 1 as a Ca<sup>2+</sup> sensor remains unclear (18). In addition to functioning in exocytosis, synaptotagmin 1 is also involved in endocytosis (19–21) possibly by virtue of its interactions with clathrin-associated adaptor molecules (22, 23).

A potential problem in labeling synapses with ECFP-fusion proteins is that such proteins may have functional effects on synapses. For example, the overexpression of wild type synaptotagmin 1 on a wild type background alters synaptic neurotransmitter release (24). To assess this possibility, we have in the present study also examined the functionality of the synaptotagmin 1-ECFP fusion protein that we are using to label presynaptic terminals. Our data demonstrate that transgenic mice expressing synaptotagmin 1-ECFP are useful tools of following presynaptic terminals *in vivo* but that the ECFP fusion inactivates synaptotagmin 1 functionally and thereby

\* The costs of publication of this article were defrayed in part by the payment of page charges. This article must therefore be hereby marked "advertisement" in accordance with 18 U.S.C. Section 1734 solely to indicate this fact.

¶¶ To whom correspondence should be addressed: Center for Basic Neuroscience, UT Southwestern, Dallas, TX 75390. Tel.: 214-648-1876; Fax: 214-648-1879; E-mail: Thomas.Sudhof@UTSouthwestern.edu.

<sup>1</sup> The abbreviations used are: GFP, green fluorescent protein; ECFP, enhanced cyan fluorescent protein; EPSC, excitatory postsynaptic current; IPSC, inhibitory postsynaptic current; SNARE, soluble NSF attachment protein receptors; AMPA,  $\alpha$ -amino-3-hydroxy-5-methyl-4-isoxazolepropionic acid; NMDA, N-methyl-D-aspartate; KO, knock-out; GST, glutathione S-transferase.

the synaptotagmin ECFP fusion protein is only a label at synapses without inserting itself as a functional component into the fusion machinery.

#### MATERIALS AND METHODS

**Animal Welfare**—All experiments involving animals performed for this study were reviewed and approved by the institutional animal use committee.

**Vector Construction**—1) The transgenic vector pThy1-Syt1-ECFP was obtained by subcloning a 3-kb XhoI-XhoI fragment from pCMV5-Syt1-ECFP-wp (24) into the XhoI site of the Thy1 minigene vector (generous gift of Dr. M. Goedert, MRC Laboratory Cambridge, UK) that contains the *Thy1* genes without exon 3 and flanking introns to achieve neuron-specific expression (25–27). 2) The Semliki Forest virus vector pSFV-Syt1-ECFP was made by inserting a 2-kb XhoI-XmaI of pCMV5-Syt1-ECFP into pSFV-wp by blunt end ligation. pSFV-wp and pSFV-Syt1 were described previously (24). 3) GST fusion vectors pGEX-Syt1-C<sub>2</sub>AB-ECFP were made by cloning a 1-kb Eco47 III-XbaI fragment of pCMV5-Syt1-ECFP into the same sites of pGEX-Syt1-C<sub>2</sub>AB. pGEX-Syt1-C<sub>2</sub>B-ECFP was produced by cloning a 1-kb Eco47 III-Eco47 III fragment into the EcoRI site of pGEX-KG by blunt end ligation.

**Generation of Transgenic Mice**—Transgenic mice were generated by injection of gel-purified pThy1-Syt1-ECFP DNA into fertilized oocytes using standard techniques (28). Transgenic founders were identified by DNA dot blotting and confirmed by PCR (see below). Six founders from six injections were backcrossed to BL6SJL/F1 hybrid mice for 1–2 generations before protein and morphology analysis, and the two lines with the highest expression levels were retained for further experiments. The genotypes of transgenic mice were determined by PCR using the following primers, wh108 (TTGAGACTAAAGTCCACCGG, from synaptotagmin 1) and wh138 (CTTATCGATACGCGTGGTAC, from the linker sequence between synaptotagmin 1 and ECFP).

**PC12 Cell Culture and Transfection**—PC12 cells were maintained in RPMI medium (Invitrogen) supplemented with 5% horse serum and 10% fetal bovine serum (Invitrogen) at 37 °C and 5% CO<sub>2</sub>. BHK21 cells were maintained in minimum essential medium (Invitrogen) supplemented with 10% fetal bovine serum, nonessential amino acids, and sodium pyruvate at 37 °C and 5% CO<sub>2</sub>. For imaging, PC12 cells were plated on polylysine (Sigma, 1 mg/ml in 0.1 M borate buffer)-coated cover glasses (18 mm, number 1.5, VWR). One day after plating, cells were transfected with DNA plasmids using Tfx-50 (Promega). Two days after transfection, cover glasses with cells were washed in PBS, fixed in 4% paraformaldehyde, and mounted on slides for confocal imaging.

**In Vitro Transcription and Viral Preparation**—Linearized Semliki Forest virus plasmids were transcribed *in vitro*. The resulting RNA was transfected into BHK21 cells by electroporation (29). One day after transfection, cell culture media containing inactive virus were collected and frozen in aliquots. On the day of infection, thawed aliquots were activated with  $\alpha$ -chymotrypsin, and cells were infected after the addition of aprotinin to inactivate  $\alpha$ -chymotrypsin.

**Immunohistochemistry**—1) Mice were anesthetized and perfused through the heart, first with PBS and then with 4% paraformaldehyde. Brains and retinas were dissected out and post-fixed in 4% paraformaldehyde for 2–4 h. After overnight immersion in 30% sucrose, tissues were embedded in Tissue-Tek OCT compound (Ted Pella, Inc.) and processed for cryostat sectioning. For overall assessment of transgene expression in brain regions, 30- $\mu$ m sagittal cryosections were mounted on slides and sealed for imaging on a confocal microscope. To examine the synaptic localization of transgenic proteins, 10- $\mu$ m cryosections of retina or diaphragm were mounted on slides and proceeded for fluorescence labeling using standard procedure. Briefly, slides with tissue sections were blocked in PBS containing 3% goat serum and 3% dry milk for 1 h at room temperature. After blocking and permeabilization in blocking buffer containing 0.15% Triton X-100 for 30 min at room temperature, the retina sections were probed with a monoclonal antibody against Rab3A (Cl42.2, 1:1000) and Alexa 568-conjugated goat-anti-mouse IgG (1:1000, Molecular Probes), while the diaphragm sections were probed with 0.1 mg/l Alexa-594-conjugated  $\alpha$ -bungarotoxin (Molecular Probes). Cover glasses were then mounted on slides and sealed for observation. 2) To prepare the whole-mount diaphragm for neuromuscular junction imaging, the diaphragm from adult mice was dissected out without fixation, washed in PBS, incubated in PBS containing 0.1 mg/l Alexa 594-conjugated  $\alpha$ -bungarotoxin (Molecular Probes) for 30 min, washed again in PBS, and mounted on slides. Whole mounts of treated diaphragms were visualized by confocal microscopy for ECFP fluorescence (green) and Alexa 594 fluorescence (red). 3) Neuronal cultures from wild type or transgenic mouse cortices were

fixed in 4% paraformaldehyde and labeled with a monoclonal antibody against Rab3A (Cl42.2, 1:1000) and Alexa 568-conjugated goat-anti-mouse IgG (1:1000, Molecular Probes) and with a polyclonal antibody against GFP (T3743, 1:500) and Alexa 488-conjugated goat-anti-rabbit IgG (1:1000, Molecular Probes).

**Confocal Microscopy**—Confocal images were acquired on a Leica TCS2 Laser scanning confocal microscope using 10 $\times$  air, 20 $\times$  air, 63 $\times$  oil (NA1.4), or 100 $\times$  oil (NA1.4) objectives. In Fig. 2, images of A, B, C, and E were montages of up to 120 individual confocal sections that were assembled into a single image using Photoshop software (Adobe).

**Biochemical Assays**—1) All recombinant proteins were expressed as GST fusion proteins in pGEX-KG and purified essentially as described (30, 31). To remove bacterial contaminants associated with C<sub>2</sub>B-domains (32), bacterial extracts containing C<sub>2</sub>B-domain proteins were treated with 1,000 units/liter of benzonase (Novagen) for 1 h at room temperature, bound to glutathione-Sepharose (0.3 ml/liter culture), and washed with (i) 250 ml of PBS, (ii) 250 ml of 200 mM NaCl, 20 mM Tris, pH 8.0, (iii) 250 ml of 200 mM NaCl, 20 mM Tris, pH 8.0, 50 mM CaCl<sub>2</sub>, (iv) 250 ml of 200 mM NaCl, 20 mM Tris, pH 8.0, (v) 250 ml of 1 M NaCl, 10 mM Tris, pH 8.0, 1 mM EDTA, and (vi) 250 ml of PBS. 2) For brain lysate preparation, three mouse forebrains were homogenized in 11 ml of 50 mM HEPES-NaOH, pH 7.4, containing protease inhibitors, 11 ml of 50 mM HEPES-NaOH, pH 7.4, 0.2 M NaCl, and 2% Nonidet P-40 were added, and then the homogenate was extracted for 4 h at 4 °C. Insoluble material was removed from the extract by centrifugation (40 min at 100,000  $\times$  g), and MgCl<sub>2</sub> was added to 2 mM final concentration. 3) For the assays for Ca<sup>2+</sup>-dependent self-association of synaptotagmin 1, 0.5-ml aliquots of the supernatant were mixed with 0.5 ml of 2 $\times$  Ca<sup>2+</sup>-EGTA buffer (1 $\times$  = 50 mM HEPES-NaOH, pH 7.4, 0.1 M NaCl, 2 mM MgCl<sub>2</sub>, 8 mM EGTA, and 1% Nonidet P-40) containing 0 or 1 mM free CaCl<sub>2</sub>. The mixture was incubated with glutathione-Sepharose beads containing  $\sim$ 10  $\mu$ g of immobilized GST fusion proteins overnight at 4 °C with rocking. The glutathione beads were washed six times in the respective binding buffers, and resuspended in 110  $\mu$ l of 1 $\times$  SDS-PAGE sample buffer. 10  $\mu$ l of each sample was analyzed by SDS-PAGE and immunoblotting using antibodies against synaptotagmin 1 (Cl41.1), Syntaxin (HPC1), SNAP-25 (Cl71.1), and Synaptobrevin (Cl69.1). 4) Centrifugation phospholipid binding assays were carried out with purified soluble GST fusion proteins in buffer A (50 mM HEPES-NaOH, pH 6.8, 0.1 M NaCl, and 4 mM EGTA) using a centrifugation assay in which the C<sub>2</sub>-domain proteins are bound in solution to heavy liposomes at different concentrations of free Ca<sup>2+</sup> essentially as described (12, 33). After binding, liposomes are isolated by centrifugation through a sucrose cushion, and bound C<sub>2</sub>-domain proteins are precipitated, resuspended in 30  $\mu$ l of 2 $\times$  SDS sample buffer, and analyzed by SDS-PAGE and Coomassie Blue staining. 5) Syntaxin immunoprecipitations were performed with a polyclonal syntaxin 1 antibody (I378, 10  $\mu$ l of serum) attached to protein A-Sepharose (10  $\mu$ l, Pharmacia) and 500  $\mu$ l of brain lysate prepared as described above. The binding reactions were incubated at 4 °C overnight with rocking, and Sepharose beads were washed six times with 1 ml of the corresponding buffers. Proteins bound to the beads were resuspended in 50  $\mu$ l of SDS-PAGE sample buffer, and 20- $\mu$ l aliquots were analyzed by SDS-PAGE and immunoblotting using antibodies against synaptotagmin 1 (Syt 1, Cl41.1), synaptophysin (Cl7.4), Rab3A (Cl42.2), Munc18, syntaxin 1 (HPC1), SNAP-25 (Cl71.1), and complexins (L668/669).

**Electrophysiological Analyses of Cultured Hippocampal Neurons in Autapses**—Individual cultures of hippocampal neurons from all mice in a litter from heterozygous mutant/wild type synaptotagmin 1 mice were prepared at postnatal day 0 on microislands of glia cells (preplated in 10% fetal bovine serum) under conditions favoring formation of autapses and used for experiments after 10–20 days in culture. Before seeding neurons in a density of 500/cm<sup>2</sup>, the medium was exchanged to neurobasal medium A (Invitrogen) with supplement B27 (Invitrogen). Only dots containing single neurons were used. Semliki Forest virus constructs were prepared and used as described (29). Rescue experiments using wild type and ECFP-fused synaptotagmin 1 constructs were performed in parallel. The extracellular recording solution contained 140 mM NaCl, 2.4 mM KCl, 10 mM HEPES-NaOH, pH 7.3, 10 mM glucose, 4 mM CaCl<sub>2</sub>, 4 mM MgCl<sub>2</sub>, 300 mosM. Synaptic transmission was recorded in the whole-cell configuration under voltage clamp using 1–2 ms depolarizations from  $-70$  to 0 mV to induce action potentials. Hypertonic sucrose solutions contained 0.5 M sucrose in addition to the regular external solution. Patch pipette solutions included 125 mM KCl, 10 mM NaCl, 4.6 mM MgCl<sub>2</sub>, 4 mM ATP-Na<sub>2</sub>, 15 mM creatine phosphate, 20 units/ml phosphocreatine kinase, 1 mM EGTA buffer, pH 7.3, 300 mosM. Chemicals were purchased from Sigma.

**Electrophysiological Analyses of Cultured Cortical Neurons**—Corti-

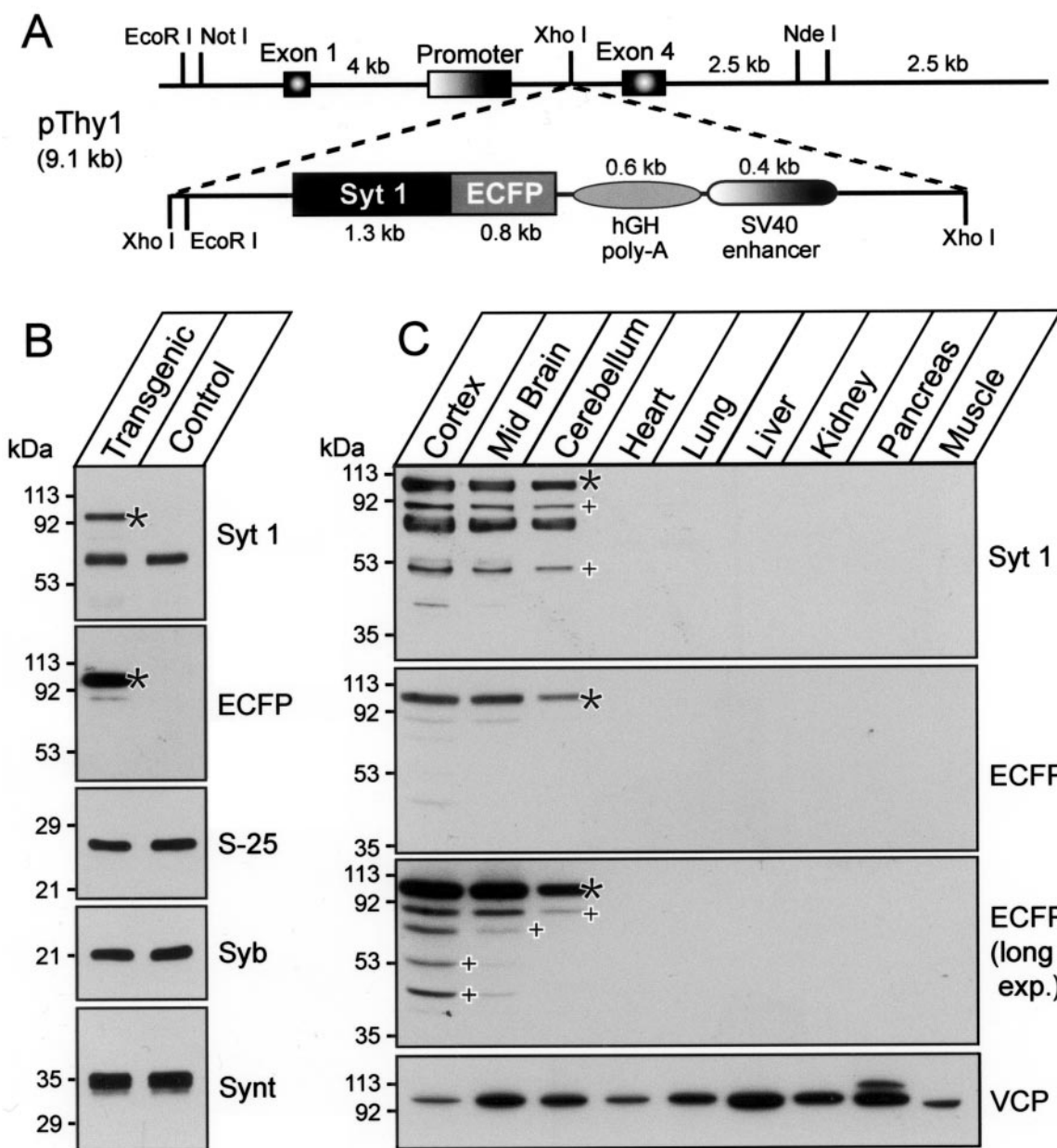


**FIG. 1. Generation of a transgenic line of mice expressing a synaptotagmin 1-ECFP fusion protein.** *A*, diagram of the transgenic vector. *B*, immunoblot analysis of synaptic proteins in transgenic and control mice. Equivalent amounts of proteins were probed with antibodies to synaptotagmin 1 (*Syt 1*), ECFP, SNAP-25 (*S-25*), synaptobrevin (*Syb*), and syntaxin 1 (*Synt*). *C*, immunoblot analysis of the expression of the transgenic protein in different mouse tissues. Equivalent amounts of protein were examined by immunoblotting with antibodies to synaptotagmin 1, ECFP, and vasolin-containing protein (*VCP*, used as a loading control). Two exposures of the ECFP blot are shown to illustrate the tissue specificity of transgene expression. In *B* and *C*, numbers on the left indicate positions of molecular weight markers, asterisks identify the transgenic synaptotagmin 1-ECFP fusion protein, and plus signs show synaptotagmin 1 breakdown products.

cal neurons were cultured from newborn mice essentially as described for hippocampal neuron culture (24) and analyzed by electrophysiology and immunocytochemistry at 14 days *in vitro*. To monitor synaptic responses, inhibitory postsynaptic currents (IPSCs) were evoked by local extracellular stimulation with a microelectrode and recorded in whole-cell mode using Multiclamp 700A amplifier (Axon Instruments Inc). The pipette solution contained 135 mM CsCl<sub>2</sub>, 10 mM HEPES, 1 mM EGTA, 4 mM Na<sub>2</sub>-ATP, 1 mM Na-GTP, 1 mM QX-314, pH 7.4. The bath solution contained 140 mM NaCl, 5 mM KCl, 2 mM CaCl<sub>2</sub>, 0.8 mM MgCl<sub>2</sub>, 10 mM HEPES, 10 mM glucose, pH 7.4. Excitatory AMPA/NMDA postsynaptic currents were blocked by addition of 50 μM AP-5 and 10 μM CNQX into bath solution. The currents were sampled at 10 kHz and analyzed using pClamp9 software (Axon Instruments Inc.).

**Miscellaneous Procedures**—Equivalent amounts of forebrain homogenates from wild type and transgenic mice were analyzed by SDS-PAGE and immunoblotting using antibodies against synaptotagmin 1 (Cl41.1), GFP (T3743), Syntaxin (HPC1), SNAP-25 (Cl71.1), and Syn-

aptobrevin (Cl69.1). For transgenic protein tissue distribution, different regions of transgenic mouse brain and various tissues were homogenized separately and quantified using BCA assay (Pierce). A similar amount of samples were analyzed by SDS-PAGE and electroblotted to Nylon membrane (Amersham Biosciences). The membranes were probed using antibodies against synaptotagmin 1 (Cl41.1), GFP (T3743), and vasolin-containing protein (K330).

## RESULTS AND DISCUSSION

**Generation of Transgenic Mice Expressing Synaptotagmin 1-ECFP**—To generate transgenic mice with fluorescent nerve terminals as a tool for studying synapse formation and function, we constructed a transgenic expression vector in which the Thy1 promoter (26) drives transcription of the coding sequence for synaptotagmin 1-ECFP (Fig. 1A). In the transgenic

vector, the synaptotagmin 1-ECFP coding sequence is followed by a polyadenylation signal from human growth hormone and the SV40 enhancer to enhance transcription (Fig. 1A). The Thy1-gene vector we used lacks exon 3 and the flanking introns to make gene expression neuron-specific (27). We injected the transgenic synaptotagmin 1-ECFP vector after removal of the vector backbone into fertilized oocytes and screened the resulting transgenic founders by DNA dot blotting (34). We then established lines from six transgenic founders by backcrossing to BL6SJL/F1 hybrid mice and analyzed the expression of synaptotagmin 1-ECFP in mouse brains from various lines by immunoblotting. In addition, we examined the location of the transgenic synaptotagmin 1-ECFP protein by fluorescence microscopy. We found that all six lines exhibited a widespread expression of synaptotagmin 1-ECFP in the brain, although the levels and precise patterns of expression varied (data not shown). For detailed studies, we selected the two lines with the highest expression levels.

We first analyzed the transgenic mice by immunoblotting. In total forebrain homogenates, immunoblotting for synaptotagmin 1 detected two bands in transgenic mice but only a single band in control mice (Fig. 1B). The upper synaptotagmin 1-reactive band in the transgenic mice (that was missing in control mice) was reactive with GFP antibodies, indicating that this band corresponds to the transgenic synaptotagmin 1-ECFP (Fig. 1B, *asterisk*). Comparison of the total immunoreactivity of endogenous synaptotagmin 1 and transgenic synaptotagmin 1-ECFP in the transgenic mice showed that the transgenic protein is expressed at slightly lower levels than the abundant endogenous synaptotagmin 1. To ensure that the overexpression of synaptotagmin 1-ECFP does not interfere with the expression of other synaptic proteins, we compared the levels of the three major synaptic SNARE proteins (SNAP-25, Synaptobrevin, and syntaxin 1) between transgenic and control mice but observed no major difference (Fig. 1B).

We next probed the tissue specificity of transgene expression (Fig. 1C). Among the tissues investigated, both endogenous synaptotagmin 1 and transgenic synaptotagmin 1-ECFP (Fig. 1C, marked with an *asterisk*) were only detectable in brain. Even prolonged exposure did not uncover an ECFP signal in non-neuronal tissues (Fig. 1C). Synaptotagmin 1 is very sensitive to proteolysis at a position in the linker between the transmembrane region and the first C<sub>2</sub>-domain (35). Multiple breakdown products of endogenous and of transgenic synaptotagmin 1 were observed (Fig. 1C, marked by *plus signs*; see in particular long ECFP exposure) that were absent when fresh brain tissue was dissolved in SDS sample buffer without dissection of brain regions as performed in Fig. 1B. Protein loads were controlled for by immunoblotting with a ubiquitously expressed marker protein, vasolin-containing protein.

**Widespread Expression of Transgenic Synaptotagmin 1-ECFP in Brain**—We next examined brain sections from the transgenic mice by fluorescence microscopy. We found that synaptotagmin 1-ECFP was expressed in most regions of the forebrain (Fig. 2A). Highest levels of synaptotagmin 1-ECFP were detected in the cortex, hippocampus, thalamus, and striatum. We observed a relatively uniform expression of synaptotagmin 1-ECFP in all regions of the thalamus (Fig. 2B). In contrast, expression in the hippocampus was heterogeneous. The mossy fiber terminals were particularly strongly labeled, whereas Schaffer collateral and dentate gyrus synapses exhibited much weaker ECFP fluorescence (Fig. 2C). The preferential labeling of mossy fiber terminals is evident from images at higher magnification that indicate a synaptic localization of synaptotagmin 1-ECFP (Fig. 2D). In the cortex, synaptotagmin 1-ECFP was also present in all layers consistent with a wide-

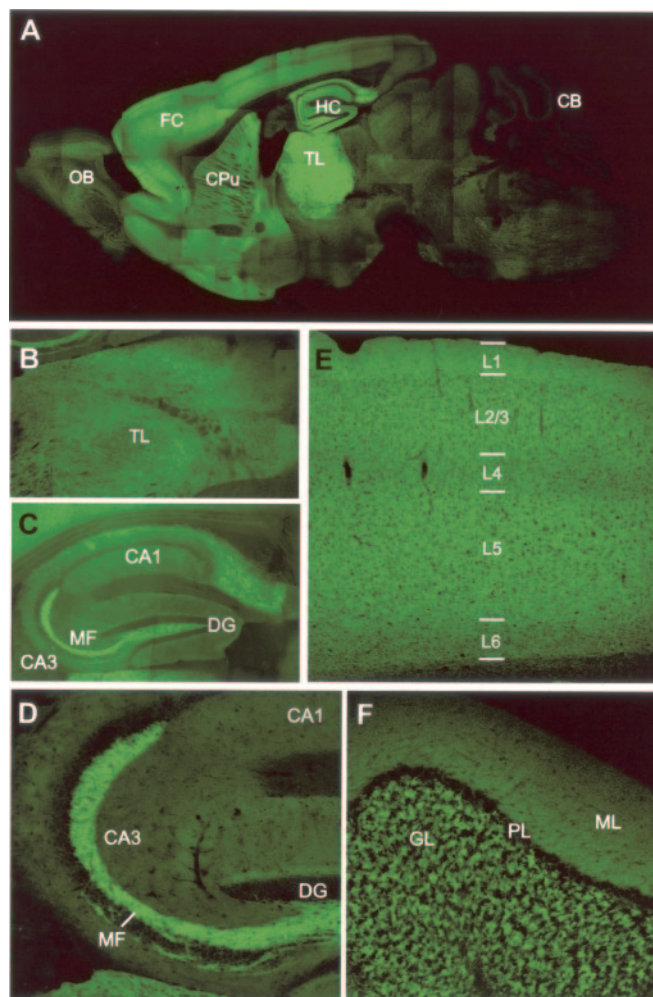
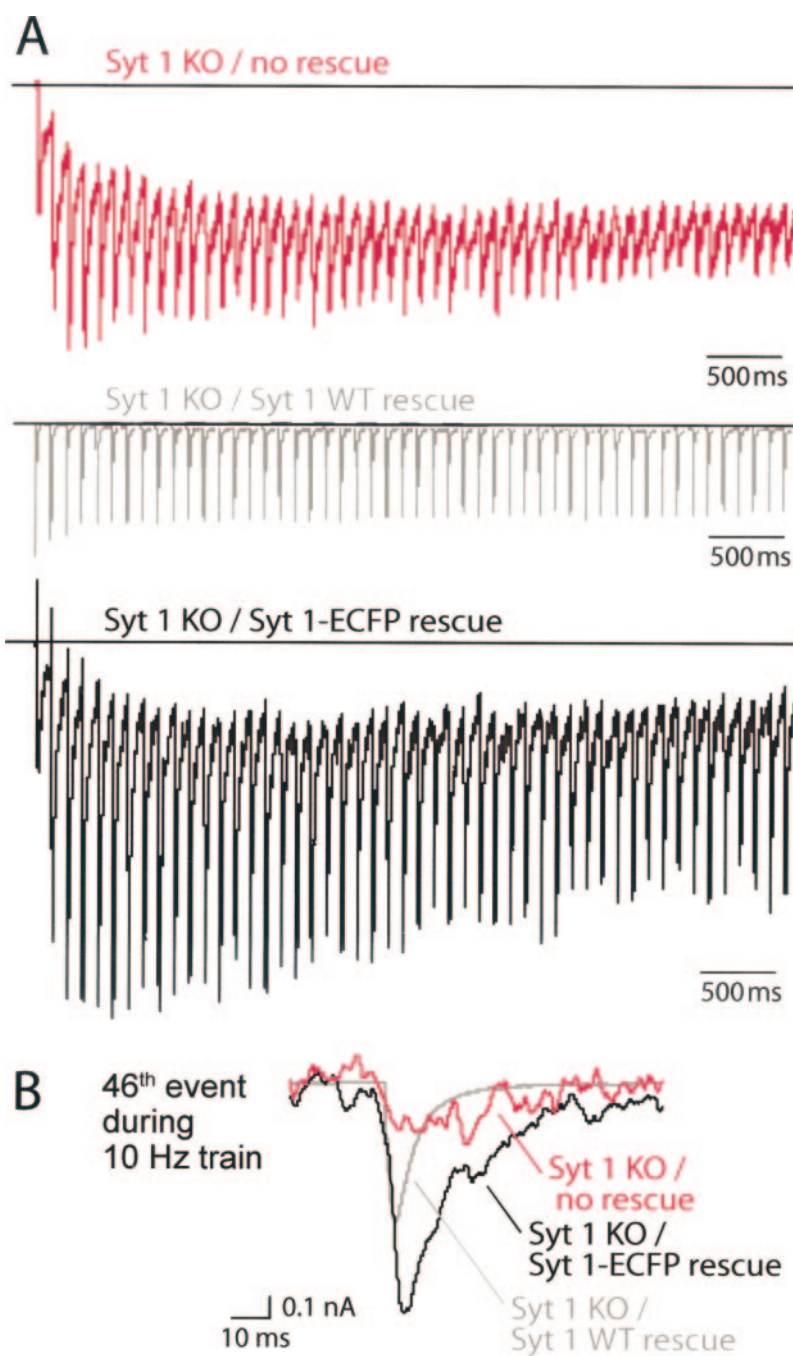


**FIG. 2. ECFP-fluorescence in different brain regions of transgenic mice expressing synaptotagmin 1-ECFP.** A, overview. B, thalamus. C, hippocampus. D, hippocampus at high magnification. E, cortex. F, cerebellum. CA1, hippocampal CA1 region; CA3, hippocampal CA3 region; CB, cerebellum; CPu, caudate putamen; DG, dentate gyrus; FC, frontal cortex; GL, cerebellar granule cell layer; HC, hippocampus; L1–L6, cerebral cortex layers 1–6; MF, hippocampus mossy fiber synapses; ML, molecular layer; OB, olfactory bulb; PL, Purkinje cell layer; TL, thalamus. No ECFP signal was observed in control mice (data not shown).

spread expression (Fig. 2E). Even in the cerebellum, where little transgenic expression was evident from the fluorescence overviews acquired at low illumination intensity (Fig. 2A), images taken at higher magnification at high illumination intensity uncovered labeling of both the granule cell layer and the molecular layer (Fig. 2F). However, labeling in the molecular layer was weak, suggesting that transgene expression in the cerebellar granule cells was low.

**Synaptotagmin 1-ECFP Is Unable to Rescue Deletion of Synaptotagmin 1**—We next crossed the transgenic synaptotagmin 1-ECFP mice with synaptotagmin 1 KO mice (13) to test whether the transgenic protein could rescue the deletion phenotype. However, transgenic synaptotagmin 1-ECFP had no beneficial effect on the survival of synaptotagmin 1 KO mice, and electrophysiological recordings from cultured hippocampal neurons of transgenic mice failed to detect an improvement of the KO phenotype (data not shown). This indicated that synaptotagmin 1-ECFP may either be expressed at levels too low in the transgenic neurons to rescue the phenotype or that the C-terminal fusion of synaptotagmin 1 with ECFP inactivates synaptotagmin function.

**FIG. 3. Synaptic responses recorded from synaptotagmin 1 KO neurons that express no exogenous synaptotagmin 1 (no rescue, red), express wild type synaptotagmin 1 (Syt 1 WT rescue, gray), or express ECFP-fused synaptotagmin 1 (Syt 1-ECFP rescue, black).** A, hippocampal neurons from synaptotagmin 1 KO mice were grown in microisland cultures in which isolated neurons form autapses. Neurons were examined either without infection or 16–24 h after infection with recombinant Semliki Forest virus expressing wild type synaptotagmin 1 or the C-terminal ECFP-synaptotagmin 1 fusion protein. EPSCs were recorded in response to action potential stimulation at 10 Hz in the presence of 4 mM  $\text{Ca}^{2+}$  and 4 mM  $\text{Mg}^{2+}$ . Responses are normalized to the first EPSC. Note that naïve synaptotagmin 1 KO neurons and synaptotagmin 1 KO neurons expressing synaptotagmin 1-ECFP exhibit a similar apparent facilitation of responses indicative of a decreased release probability and a similar shift in baseline current indicative of a relative increase in asynchronous release. No rescue,  $n = 5$ ; Syt 1 WT rescue,  $n = 12$ ; Syt 1-ECFP rescue,  $n = 6$ . B, representative traces of EPSCs from the end of the 10-Hz stimulus train.



To test the functionality of synaptotagmin 1-ECFP more rigorously, we examined synaptic transmission in cultured glutamatergic hippocampal neurons from synaptotagmin 1 KO mice. Neurons were infected with recombinant Semliki Forest virus expressing either wild type synaptotagmin 1 or synaptotagmin 1-ECFP. Neurons expressing wild type synaptotagmin 1 were identified on the basis of the fluorescence of GFP that is encoded in the recombinant virus via an internal ribosome entry site sequence, whereas neurons expressing synaptotagmin 1-ECFP were identified based on the ECFP fluorescence. We first used trains of action potential to assess the rescue activity mediated by synaptotagmin 1 *versus* synaptotagmin 1-ECFP (Fig. 3). In naïve (*i.e.* uninfected) synaptotagmin 1 KO neurons, excitatory postsynaptic current (EPSC) peak amplitudes evoked by a 10-Hz train were initially very small (normalized in Fig. 3), facilitated in the first few responses, and subsequently declined. At the same time, asynchronous

release became the dominant form of release as evidenced by the downward shift in baseline membrane currents (36–38). KO neurons expressing wild type synaptotagmin 1 displayed a completely different behavior that was similar to that of wild type neurons (Fig. 3 and data not shown); neurotransmitter release remained highly synchronous throughout the 10-Hz train, whereas the peak amplitudes exhibited a moderate decline, and the baseline membrane currents remained low. In contrast, KO neurons expressing synaptotagmin 1-ECFP exhibited properties similar to those of naïve KO neurons; peak amplitudes were small and declined during the 10-Hz stimulus train, whereas asynchronous release remained a major component of synaptic transmission as evidenced by the shift in baseline membrane current (Fig. 3). This indicates that synaptotagmin 1-ECFP, even when over-expressed, is not able to fully rescue the synaptotagmin 1 KO phenotype.

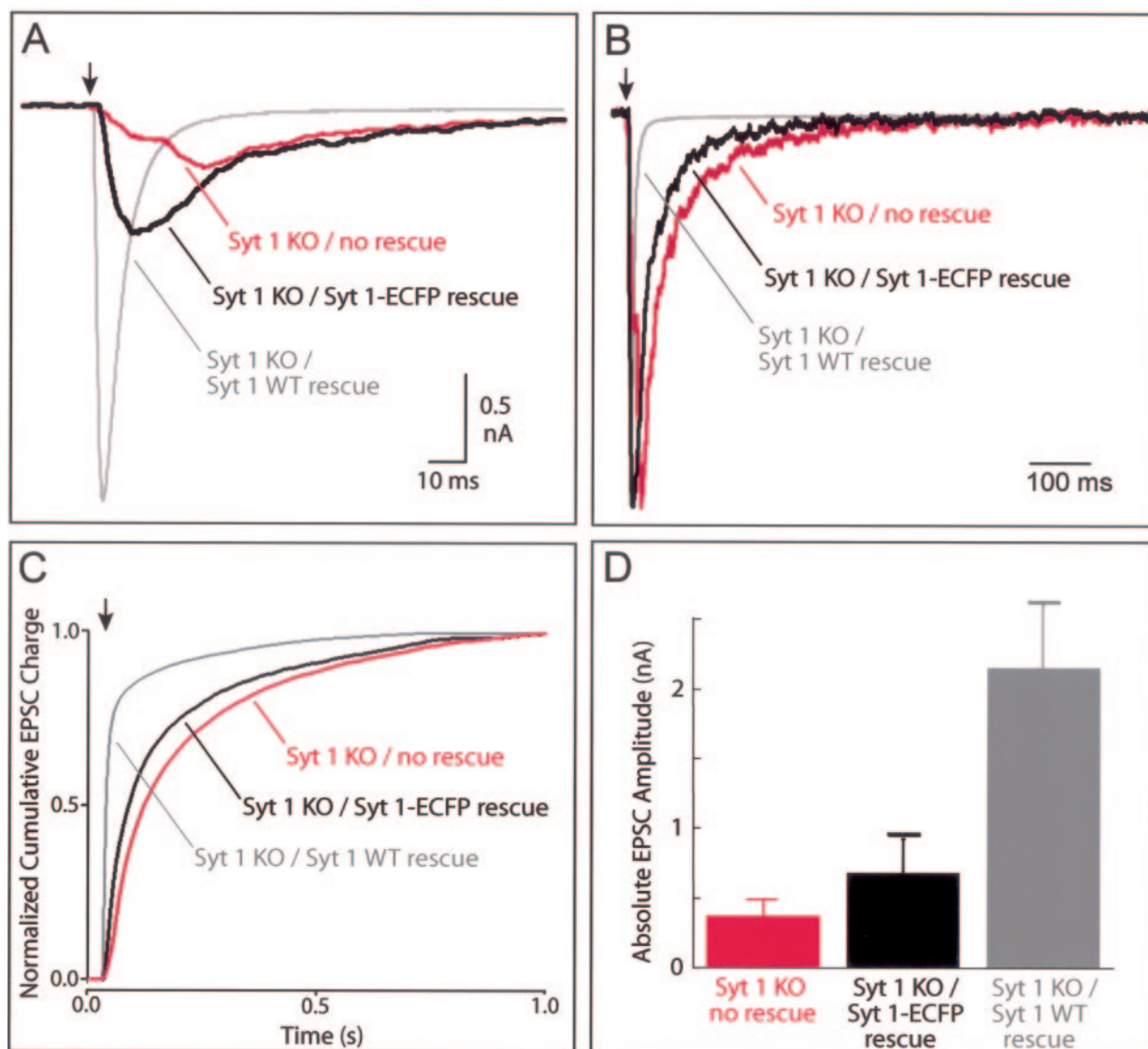


**FIG. 4. C-terminal ECFP fusion to synaptotagmin 1 impairs the ability of synaptotagmin 1 to rescue the fast time course of  $\text{Ca}^{2+}$ -triggered release in synaptotagmin 1 KO neurons.** *A*, sample traces of EPSCs recorded in autaptic hippocampal neurons from synaptotagmin 1 KO mice (*Syt 1 KO*) that either do not express exogenous synaptotagmin 1 (*red, no rescue*), were infected with Semliki forest virus producing wild type synaptotagmin 1 (*gray, Syt 1 WT rescue*), or with virus producing synaptotagmin 1-ECFP (*black, Syt 1-ECFP rescue*). EPSCs were elicited by action potentials (*arrow*). *B*, averaged EPSCs from multiple synaptotagmin 1 KO neurons that either do not express exogenous synaptotagmin 1 (*red*), express wild type (*gray*), or express ECFP-fused synaptotagmin 1 (*black*). EPSCs are normalized to their maximal amplitude to illustrate their differential kinetics. *C*, time course of the normalized total release in response to stimulation by action potentials. EPSC charges from synaptotagmin 1 KO neurons that either do not express exogenous synaptotagmin 1 (*red*) or express wild type (*gray*) or ECFP-fused synaptotagmin 1 (*black*) were integrated and averaged over 1 s. *D*, peak average amplitudes of EPSCs recorded in synaptotagmin 1 KO neurons that either do not express exogenous synaptotagmin 1 (*red*) or express wild type (*gray*) or ECFP-fused synaptotagmin 1 (*black*). Data in *C–D* are from 5 naïve synaptotagmin 1 KO neurons, 12 wild type synaptotagmin 1 rescue neurons, and 6 synaptotagmin 1-ECFP rescue neurons. Error bars in *D* show S.E.

To fully characterize how much of a rescue the synaptotagmin 1-ECFP fusion protein is able to mediate, we examined the time course of release triggered by low-frequency action potentials in synaptotagmin 1 KO neurons that either express no exogenous synaptotagmin 1 (“naïve” neurons) or that express wild type or ECFP-fused synaptotagmin 1 (Fig. 4). The peak amplitudes of the EPSCs in KO neurons expressing synaptotagmin 1-ECFP was lower than in KO neurons expressing wild type synaptotagmin 1 (Fig. 4A), and the release time course was much slower (Fig. 4B). At the same time, however, amplitudes were larger in KO neurons expressing synaptotagmin 1-ECFP than in naïve KO neurons, and the time course was faster. Thus synaptotagmin 1-ECFP mediates a partial rescue of the KO phenotype. The partial rescue of the time course is illustrated in Fig. 4C, which

shows the mean normalized charge integral of EPSCs from synaptotagmin 1 KO, synaptotagmin 1 wild type rescue, and synaptotagmin 1-ECFP rescue neurons. To estimate how much the “partial” rescue amounts to we determined the average peak amplitude in the three types of neurons, because it mainly reflects the synchronous fraction of release, as responses with predominant synchronous release time course have a large peak response (Fig. 4D). Expression of synaptotagmin 1-ECFP in synaptotagmin 1 KO neurons doubled the peak amplitude, but wild type synaptotagmin 1 expression caused a >5-fold increase. Thus the partial rescue mediated by synaptotagmin 1-ECFP accounts only for a small percentage (<20%) of wild type synaptotagmin 1 function, a surprising result considering the fact that no mutations were introduced into synaptotagmin 1 itself.

**FIG. 5. Immunocytochemical analysis of cultured cortical neurons from control mice (top) and mice carrying the synaptotagmin 1-ECFP transgene (bottom).** Neurons (14 days *in vitro*) were fixed and stained with antibodies to Rab3A (left panels, red) or ECFP (middle panels, green). The right panels exhibit the overlap between the two stains. Calibration bar in the right lower corner = 10  $\mu\text{m}$  and applies to all panels. Arrows illustrate synapses at which Rab3A and Syt1-ECFP are colocalized.

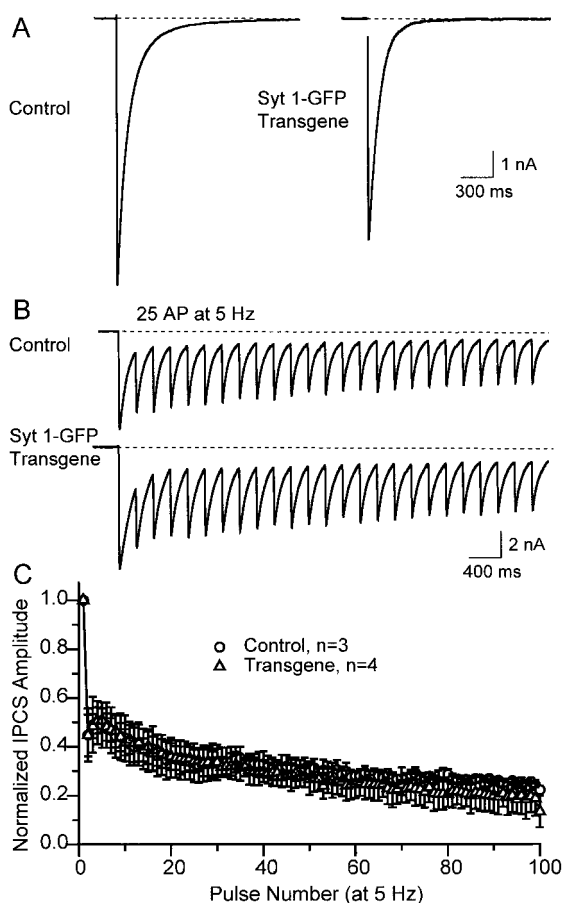
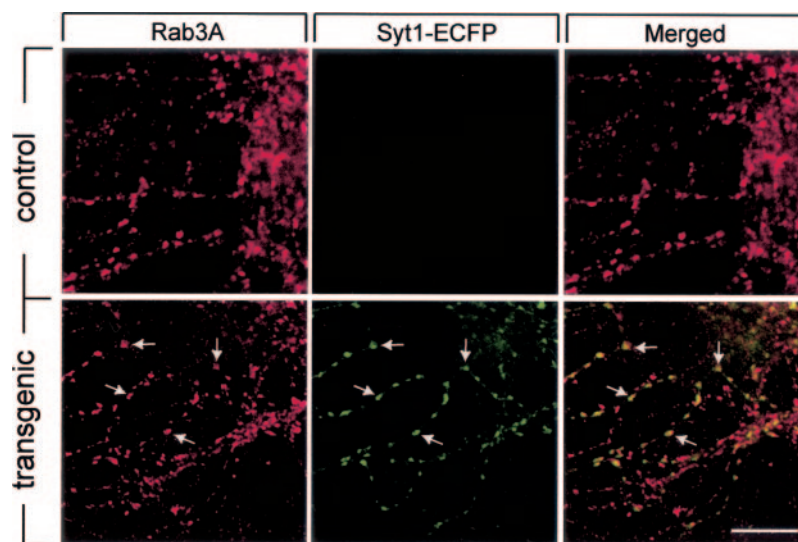


**FIG. 6. Comparison of evoked synaptic responses monitored in control mice and in wild type mice carrying the synaptotagmin 1-ECFP transgene.** *A*, representative IPSCs recorded in cortical neurons cultured from newborn control or synaptotagmin 1-ECFP transgenic mice and analyzed 14 days *in vitro*. Responses were monitored during action potentials delivered at 0.1 Hz at a holding potential of  $-70$  mV. No consistent difference between control and transgenic neurons was observed. *B*, traces of IPSCs recorded from control or synaptotagmin 1-ECFP transgenic cortical neurons in response to 25 action potentials delivered at 5 Hz at a holding potential of  $-70$  mV. *C*, normalized average amplitudes of IPSCs evoked by 100 action potentials delivered at 5 Hz (data shown are means  $\pm$  S.E.).

*Transgenic Synaptotagmin 1-ECFP Is Expressed Only in Synapses but Has No Major Effect on Synaptic Responses in Wild Type Mice*—We next asked whether the synaptotagmin

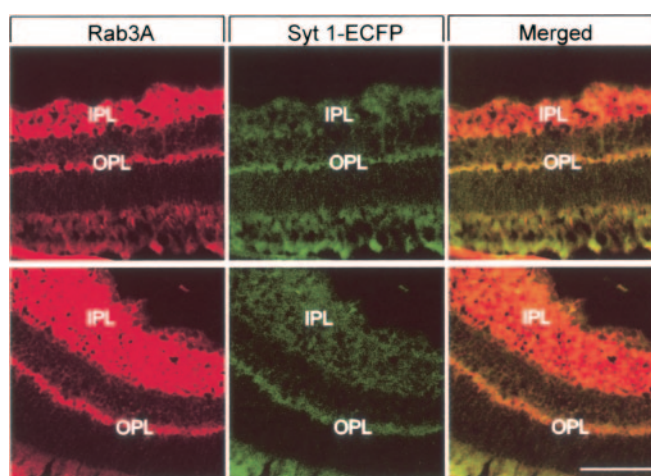


**FIG. 7. Double labeling of retina sections from transgenic mice expressing synaptotagmin 1-ECFP.** Two independent views. Note that synaptotagmin 1-ECFP signal is relatively sparse in the inner plexiform layer (IPL) but strong in the outer plexiform layer (OPL). Signal at the bottom is nonspecific autofluorescence from the retinal pigment epithelium. No ECFP signal was observed in control mice (data not shown). Calibration bar in the right lower corner = 100  $\mu\text{m}$  and applies to all panels.

1-ECFP fusion protein, as expressed in the neurons of transgenic mice, could have a major dominant-negative effect on synaptic transmission in these mice. Such an effect may not necessarily be apparent from the fact that the transgenic mice are viable and fertile, because other mice that exhibit major changes in synaptic transmission (e.g. RIM1 $\alpha$  knock-out mice or synaptotagmin 1-R233Q mutant mice; see Refs. 16 and 39) are also viable and fertile. To address this possibility, we cultured cortical neurons from newborn transgenic wild type and littermate non-transgenic control mice. We first examined the localization of the synaptotagmin 1-ECFP fusion protein in these neurons by immunocytochemistry (Fig. 5). We found that the synaptotagmin 1-ECFP fusion protein, identified via its ECFP moiety, was highly enriched in synapses; no signal was detected in neurons from control mice.

We next analyzed the properties of IPSCs recorded from the cultured cortical neurons. IPSCs were evoked by local extracellular stimulation in the presence of AMPA/NMDA receptor blockers and recorded in whole-cell mode. In control experiments, the addition of picrotoxin (200  $\mu\text{M}$ ) to the bath solution resulted in complete block of evoked responses, suggesting that

**FIG. 8. Double labeling of neuromuscular junctions from transgenic mice expressing synaptotagmin 1-ECFP.** Whole mounts (*A* and *B*) and 10- $\mu\text{m}$  cryosections (*C* and *D*) of neuromuscular junctions from the diaphragm were labeled with Alexa 594-conjugated  $\alpha$ -bungarotoxin, and visualized by confocal microscopy for ECFP fluorescence (green) and Alexa 594 fluorescence (red). No ECFP signal was observed in control mice (data not shown). *A* and *B* exhibit a view from the top onto the muscle, and *C* and *D* show a section through the neuromuscular junction. Calibration bar (10  $\mu\text{m}$ ) in *B* applies to *A* and *B* and that in *D* to *C* and *D*.

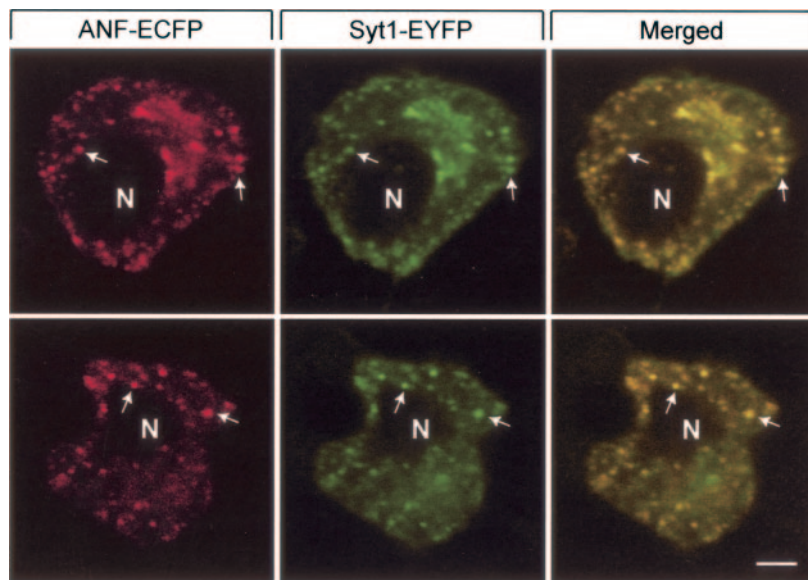
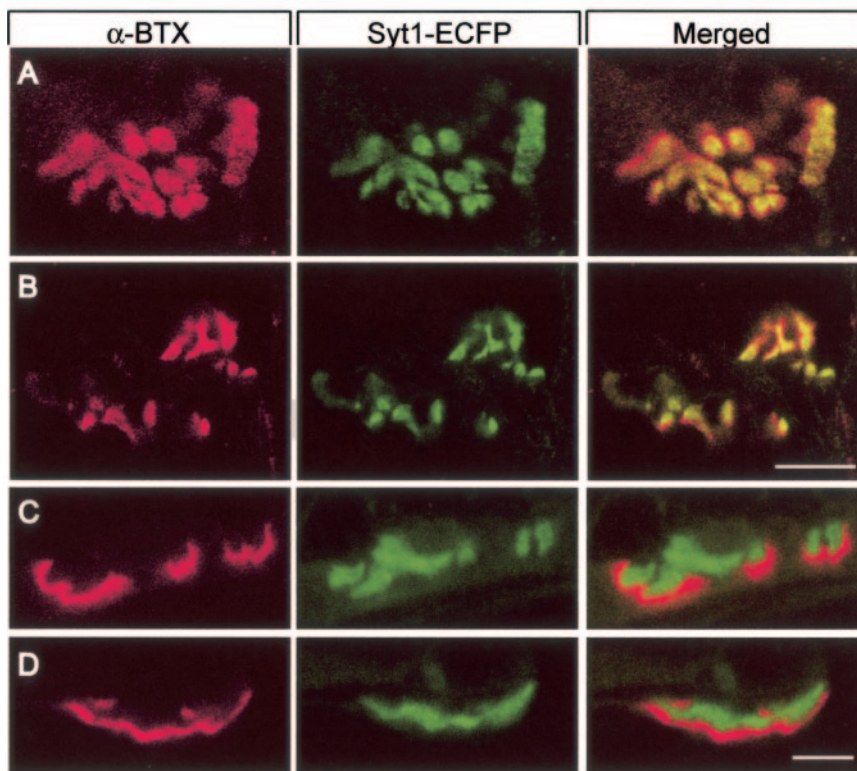


**FIG. 9. Analysis of the localization of synaptotagmin 1-ECFP in transfected PC12 cells.** Pictures show two examples of confocal images of PC12 cells that co-express an ECFP fusion protein of atrial natriuretic factor (ANF-ECFP, red) and Syt1-EYFP (green). Calibration bar = 2  $\mu\text{m}$ ; N, nucleus. Arrows indicate vesicles at which ANF-ECFP and Syt1-EYFP are colocalized.

recorded IPSCs were primarily mediated by activation of  $\gamma$ -aminobutyric acid receptors (data not shown). The absolute amplitudes of the IPSCs recorded from control or synaptotagmin 1-ECFP transgenic cultures in response to action potentials delivered at 0.1 Hz were similar in size (wild type =  $4.9 \pm 1.6$  nA,  $n = 4$ ; transgene =  $4.7 \pm 0.8$  nA,  $n = 5$ ; mean  $\pm$  S.D.) and kinetics (Fig. 6*A*). To search for potential changes in release probability or vesicle recycling, we subsequently tested synaptic IPSCs evoked by repeated action potentials applied at higher frequency. The kinetics with which use-dependent depression develops at a synapse and the amount of steady-state depression at a given stimulation frequency are sensitive but indirect measures of the release probability and vesicle recycling at a synapse (40). However, we found no significant differences in the depression of IPSCs evoked by repetitive stim-

ulation at 5 Hz (Fig. 6, *B* and *C*). Thus, overexpression of synaptotagmin 1-ECFP does not have a major overriding effect on the synchronous component of synaptic transmission as measured in these cortical inhibitory synapses.

**Synaptic Localization of Fluorescent Synaptotagmin 1-ECFP**—A potential explanation for the lack of rescue by synaptotagmin 1-ECFP is that the ECFP fusion protein is not transported to the synapses. To test this, we examined the localization of synaptotagmin 1-ECFP. The enrichment of synaptotagmin 1-ECFP in mossy fiber terminals (Fig. 2*D*) and the punctate labeling of the granule cell layer in the transgenic mice (Fig. 2*F*) strongly suggest a synaptic localization. This was confirmed in an analysis of cultured neurons from synaptotagmin 1-ECFP transgenic mice (Fig. 5), of sections of transgenic retina where synapses form a single contiguous band in



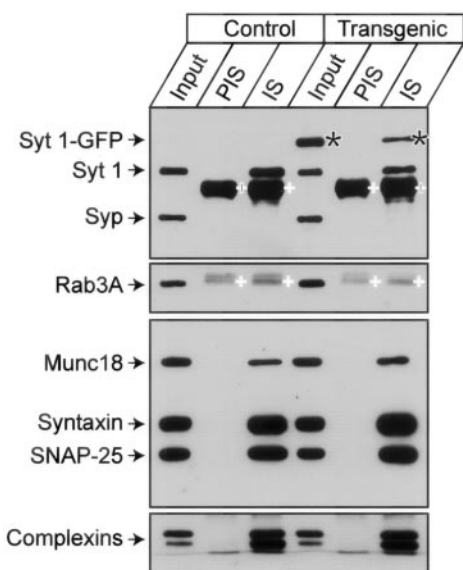


**FIG. 10. Binding of synaptotagmin 1-ECFP to SNARE complexes.** Immunoprecipitations were performed with proteins from detergent-solubilized brain extracts from control and synaptotagmin 1-ECFP transgenic mice. The panels display representative immunoblots of the starting materials (*Input*) and the immunoprecipitates obtained with preimmune serum (*PIS*) or a syntaxin 1 immune serum (*IS*). Precipitates were examined by immunoblotting for synaptotagmin 1 (*Syt 1*), syntaxin 1, SNAP-25, complexins, synaptophysin, Munc18, and Rab3A. Asterisks indicate the position of the synaptotagmin 1-ECFP fusion protein; plus signs denote cross-reactive bands corresponding to the heavy and light chains of the immunoglobulins used during the immunoprecipitations.

the outer plexiform layer (Fig. 7), and whole mounts of neuromuscular junctions where nerve terminals can be directly visualized (Fig. 8). Double labeling experiments in cultured neurons and the retina revealed that the localization of transgenic synaptotagmin 1-ECFP precisely coincides with that of Rab3A, a synaptic vesicle protein (Figs. 5 and 7). In the retina, both synaptotagmin 1-ECFP and Rab3A were detectable in the outer plexiform layer that is primarily composed of photoreceptor synapses and in the more broad inner plexiform layer that contains multiple layers of synapses. Both proteins were absent from other layers of the retina. Similarly, we observed that synaptotagmin 1-ECFP was highly enriched in neuromuscular nerve terminals opposite from the sites that are labeled with  $\alpha$ -bungarotoxin (Fig. 8, A and B). To ensure that the labeling observed does not correspond to the presence of synaptotagmin 1-ECFP in the postsynaptic muscle cell, we also optically analyzed cross-sections of the neuromuscular junctions and found that the synaptotagmin 1-ECFP signal was unequivocally restricted to the presynaptic terminals above the  $\alpha$ -bungarotoxin-positive postsynaptic specializations (Fig. 8, C and D).

We next asked whether synaptotagmin 1-ECFP is actually deposited into secretory vesicles. Because the small size of synaptic vesicles makes it difficult to address this question in neurons, we examined transfected neuroendocrine PC12 cells similar to the experiments that we had earlier performed to study the targeting of synaptotagmin 1 (24). As shown in Fig. 9, we found that synaptotagmin 1-EYFP completely co-localized with co-transfected ANF-EYFP, a marker of secretory vesicles (41). These results are consistent with a selective synaptic localization of transgenic synaptotagmin 1-ECFP.

**Biochemical Properties of the Synaptotagmin 1-GFP Fusion Protein**—The synaptic localization but non-functionality of synaptotagmin 1-ECFP suggests that either the ECFP-fusion impairs the biochemical activity of synaptotagmin 1 or that the simple addition of a bulky protein moiety at the C terminus of

synaptotagmin 1 prevents its normal function. To distinguish between these two possibilities, we measured the three principal properties of synaptotagmin 1 that have been associated with its role in triggering vesicle exocytosis, binding to SNARE complexes (42–48), to phospholipids (10–12), and to itself (49–51).

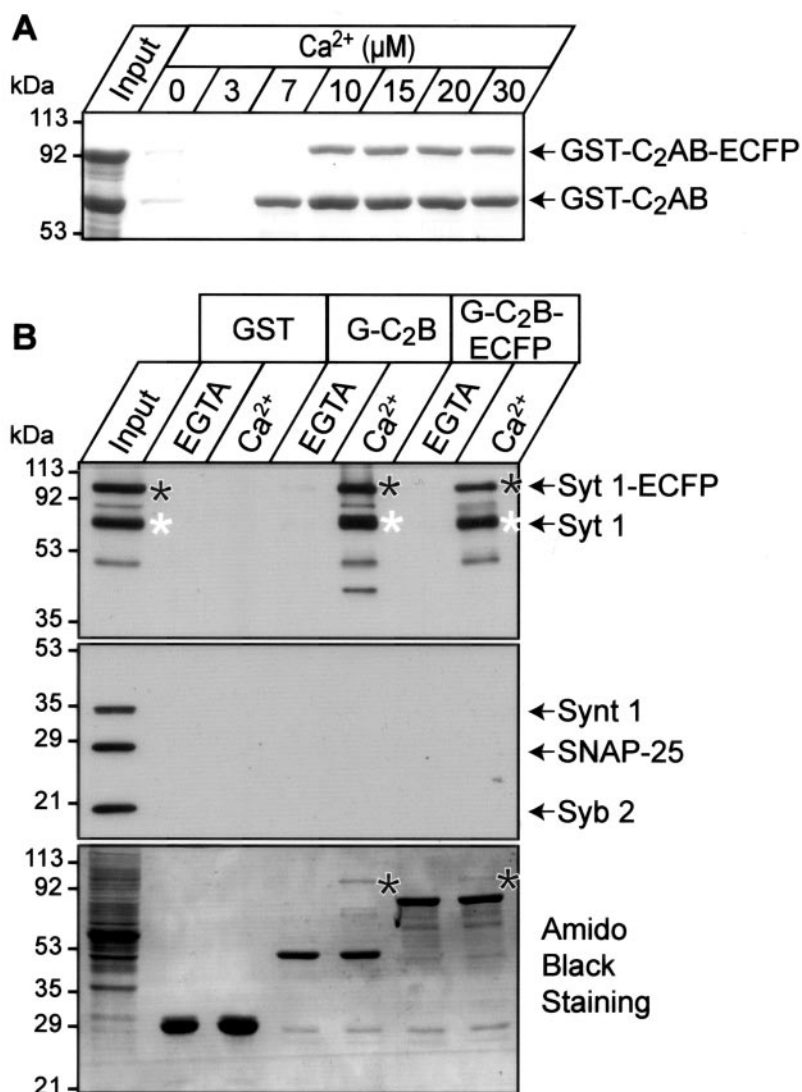
We first examined the  $\text{Ca}^{2+}$ -independent binding of synaptotagmin 1 to SNARE complexes (Fig. 10). We did not study  $\text{Ca}^{2+}$ -dependent binding, because previous experiments suggested that  $\text{Ca}^{2+}$ -dependent SNARE binding may not be absolutely essential for triggering exocytosis, although it may contribute to the regulation of exocytosis (47). To assess SNARE complex binding, we immunoprecipitated proteins from mouse brain homogenates that were prepared under conditions favoring SNARE complex assembly. We immunoprecipitated proteins with syntaxin 1 preimmune or immune serum and then analyzed bound proteins by immunoblotting. SNARE complexes were immunoprecipitated from transgenic and from naive non-transgenic control brains. We found that as expected for SNARE complexes, SNAP-25 and complexin were efficiently co-immunoprecipitated with syntaxin 1 (Fig. 10). The immunoprecipitations were specific, because preimmune serum was inactive, and because unrelated proteins such as synaptophysin or Rab3A were not brought down. Both unmodified synaptotagmin 1 and synaptotagmin 1-ECFP were efficiently co-immunoprecipitated with syntaxin 1 indicating that both were able to associate with the SNARE complex (Fig. 10). Note, however, that although the co-immunoprecipitation of synaptotagmin 1 with the SNARE complexes is specific, relatively less synaptotagmin 1 than other SNAREs or complexin is co-immunoprecipitated with syntaxin 1.

We next investigated  $\text{Ca}^{2+}$ -dependent phospholipid binding (Fig. 11A). Using recombinant double  $\text{C}_2$ -domain fragments from synaptotagmin 1 that contain or lack the C-terminal ECFP fusion, we found that both efficiently bound to negatively charged liposomes as described previously for the unfused double  $\text{C}_2$ -domain fragment (52). However, the apparent  $\text{Ca}^{2+}$  affinity of the ECFP fusion protein was slightly lower than that of the unfused protein (Fig. 11A). Although this shift, which approximates that of the R233Q mutation (16), cannot explain the lack of functionality of synaptotagmin 1-ECFP, it does highlight the distinct sensitivity of the properties of the double  $\text{C}_2$ -domain fragment to modifications on its domains.

Finally, we tested the ability of synaptotagmin 1 to interact with itself in a  $\text{Ca}^{2+}$ -dependent manner (Fig. 11B). The nature of this activity is uncertain and its relevance questionable, although it suggests a potential mechanism by which synaptotagmin polymerization could participate in fusion pore opening (47–49). We found that synaptotagmin 1-ECFP was equally well pulled down in a  $\text{Ca}^{2+}$ -dependent manner by GST fusion proteins of the synaptotagmin 1  $\text{C}_2$ B-domain as unfused synaptotagmin 1. The GST- $\text{C}_2$ B-domain in turn was equally effective in pulling down naive synaptotagmin 1 or synaptotagmin 1-ECFP, either without itself being fused to ECFP or after it was fused to ECFP (Fig. 11B). The  $\text{Ca}^{2+}$ -dependent pull downs were so effective that the brain synaptotagmins could be detected by Amido Black staining of the blotting membranes. Together these experiments unequivocally demonstrated that synaptotagmin 1-ECFP is able to participate in the major biochemical interactions that have been identified for synaptotagmin 1 thus indicating that the ECFP fusion impairs synaptotagmin 1 function by spatial interference.

**Summary**—Here, we report the generation of transgenic mice that express ECFP-tagged synaptotagmin 1 in central synapses. The ECFP-tagged synaptotagmin 1 provides an *in vivo* stain of the terminals that complements existing mice in

**FIG. 11. Biochemical properties of synaptotagmin 1-ECFP.** **A**, phospholipid binding. Sucrose-filled heavy liposomes composed of 25% phosphatidylserine and 75% phosphatidylcholine were incubated with purified GST fusion proteins in solutions containing free  $\text{Ca}^{2+}$  as indicated using Ca-EGTA buffers. Liposomes were washed, and bound proteins were examined by SDS-PAGE and Coomassie staining. **B**,  $\text{Ca}^{2+}$ -dependent self-association. Detergent-solubilized brain extracts from transgenic mice expressing synaptotagmin 1-ECFP were mixed with equal volumes of  $2\times \text{Ca}^{2+}$ -EGTA buffer (see "Materials and Methods") containing 0 or 1 mM free  $\text{Ca}^{2+}$  and incubated with glutathione-Sepharose beads containing  $\sim 10 \mu\text{g}$  immobilized GST fusion proteins overnight at  $4^\circ\text{C}$ . After washing, bound proteins were eluted from the beads with SDS-PAGE sample buffer and analyzed by SDS-PAGE and immunoblotting using antibodies against synaptotagmin 1, Syntaxin, SNAP-25, and Synaptobrevin. Synaptotagmin 1-ECFP is marked with a *black asterisk*, and endogenous non-transgenic synaptotagmin 1 is marked with a *white asterisk*. Note the fact that the synaptotagmin 1-ECFP fusion protein can be seen on the Amido Black-stained membrane.



which subsets of neurons are filled with transgenically expressed uniformly distributed GFP derivatives (4, 5). These mice may be useful for experiments in which fluorescent synapses will allow monitoring synaptogenesis and synaptic remodeling (4, 6, 7) and help following pathological changes in synapses in mouse models of human disease (53).

Our data demonstrated that transgenic synaptotagmin 1-ECFP, when expressed under control of the Thy1 promoter (27), is widely present in synapses throughout the brain (Figs. 1, 2, 5, 7, and 8) and is targeted to secretory vesicles at least in transfected cells (Fig. 9). The transgenically expressed synaptotagmin 1-ECFP failed to rescue the lethal synaptotagmin 1 KO phenotype. This finding indicated that the ECFP fusion may have inactivated synaptotagmin 1 function while retaining its normal localization. Indeed, we confirmed by using overexpression of wild type and ECFP-fused synaptotagmin 1 in cultured neurons from synaptotagmin 1 KO mice that the synaptotagmin 1-ECFP fusion protein was unable to perform the normal  $\text{Ca}^{2+}$ -sensor function of synaptotagmin 1 in neurotransmitter release (Figs. 3 and 4). This was unexpected because in *Drosophila*, a C-terminal fusion protein of synaptotagmin 1 that contains a shorter attached sequence, a sequence that includes a tetracysteine motif for *in vivo* labeling with biarsenical dyes, was fully active (21). It is possible that the *Drosophila* synaptotagmin 1-fusion proteins were still active, because a much shorter sequence was

fused to synaptotagmin 1 than the ECFP studied here.

In our biochemical experiments, we observed that the activities of the synaptotagmin 1-ECFP fusion protein were not dramatically altered (Figs. 10 and 11). Our current model of how synaptotagmin 1 functions in fusion, derived from a series of experiments in multiple laboratories (reviewed in Ref. 54) is depicted in the model in Fig. 12. According to this model, synaptotagmin 1 associates SNARE complexes that have formed during priming of synaptic vesicles for release in a  $\text{Ca}^{2+}$ -independent manner. When release is triggered, synaptotagmin 1 binds  $\text{Ca}^{2+}$  and phospholipids and thereby perturbs an unstable phospholipid intermediate that was established by SNARE complex assembly. This model provides a ready explanation for why the synaptotagmin 1-ECFP fusion protein may be inactive (Fig. 12). In the model, synaptotagmin 1 has to fit into a relatively constrained space in association with SNARE complexes on docked and primed vesicles. A plausible hypothesis is that the ECFP, when attached to synaptotagmin 1, makes it impossible for synaptotagmin 1 to fit into this space, and thereby prevents synaptotagmin 1 from functioning properly. Although at present this is the most parsimonious hypothesis to explain our data, alternative explanations, for example that the ECFP fusion prevents an as yet unknown binding reaction by synaptotagmin 1, cannot be excluded.

Independent of the reason for the functional inactivity of the synaptotagmin 1-ECFP fusion protein, a positive outcome of

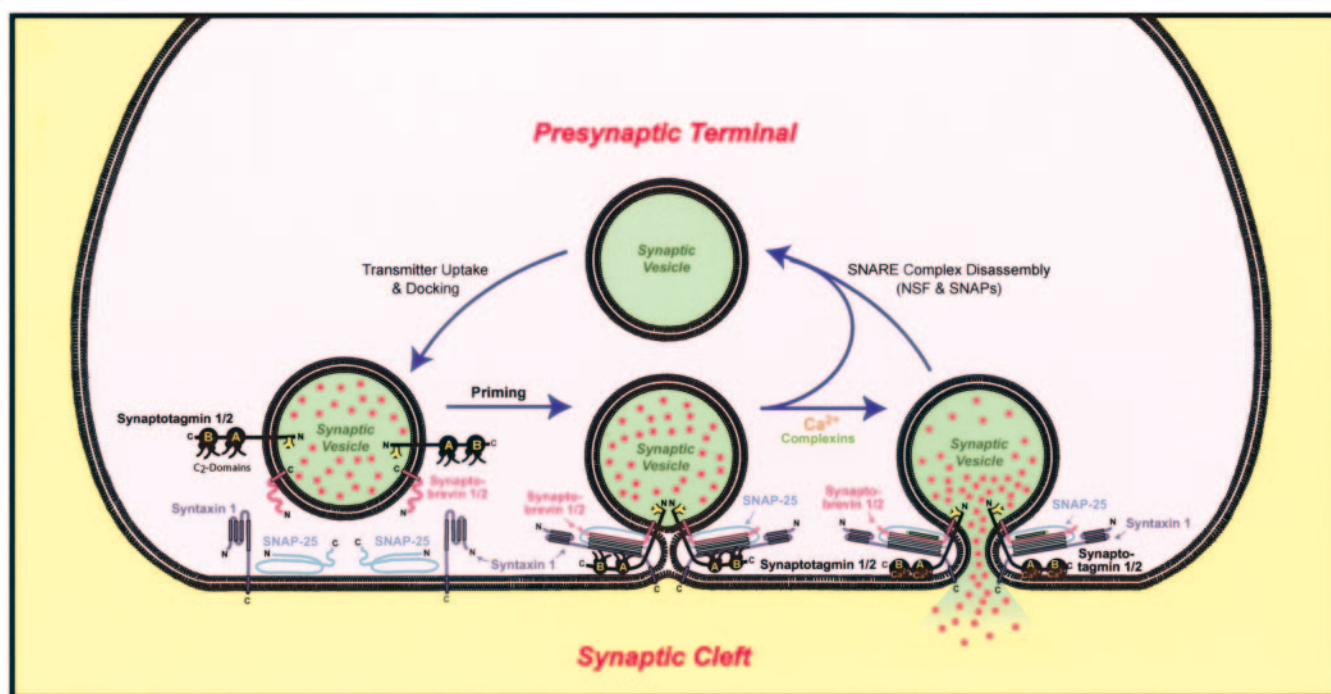


FIG. 12. **Model of synaptotagmin 1 function in  $\text{Ca}^{2+}$ -triggering of neurotransmitter release.** Synaptic vesicles are proposed to be docked to the active zone by an unknown mechanism (*left*), then SNARE complexes are assembled during priming, and synaptotagmin 1 binds to the assembled complexes in a  $\text{Ca}^{2+}$ -independent manner (*center*), and finally  $\text{Ca}^{2+}$  influx induces neurotransmitter release by opening the fusion pore in a process that is triggered by the  $\text{Ca}^{2+}$ -dependent insertion of synaptotagmin 1  $\text{C}_2$ -domains into the phospholipid bilayer (*right*). The fusion pore opening is proposed to be a purely physicochemical process fueled by the destabilization of the double bilayer structure induced by SNARE complex assembly. The model predicts that the release machinery surrounding the emerging fusion pore operates under tight spatial constraints, suggesting that any bulky moieties attached to synaptotagmin 1 or other components of the machinery may interfere with their positioning in the restricted space in which this machinery operates (model adapted from Ref. 54).

this functional inactivity is that synaptotagmin 1-ECFP is unlikely to interfere with the normal function of synaptotagmin 1 in synapses. Thus as an *in vivo* stain for synapses, the synaptotagmin 1-ECFP protein is innocuous and does not influence the very structure it is marking. This increases the usefulness of synaptotagmin 1-ECFP over, for example, synaptophysin-ECFP fusion proteins which inhibit exocytosis<sup>2</sup> and should make the transgenic mice reported here useful for many experiments in different laboratories.

**Acknowledgments**—We thank I. Leznicki, A. Roth, Nicole Hamlin, and E. Borowicz for technical assistance, and Drs. M. Goedert (Cambridge) and R. Jahn (Goettingen) for the gift of reagents.

#### REFERENCES

- Foeller, E., and Feldman, D. E. (2004) *Curr. Opin. Neurobiol.* **14**, 89–95
- Kauer, J. A. (2004) *Annu. Rev. Physiol.* **66**, 447–475
- Inoue, A., and Okabe, S. (2003) *Curr. Opin. Neurobiol.* **13**, 332–340
- De Paola, V., Arber, S., and Caroni, P. (2003) *Nat. Neurosci.* **6**, 491–500
- Feng, G., Mellor, R. H., Bernstein, M., Keller-Peck, C., Nguyen, Q. T., Wallace, M., Nerbonne, J. M., Lichtman, J. W., and Sanes, J. R. (2000) *Neuron* **28**, 41–51
- Grutzendler, J., Kasthuri, N., and Gan, W. B. (2002) *Nature* **420**, 812–816
- Trachtenberg, J. T., Chen, B. E., Knott, G. W., Feng, G., Sanes, J. R., Welker, E., and Svoboda, K. (2002) *Nature* **420**, 788–794
- Perin, M. S., Fried, V. A., Mignery, G. A., Jahn, R., and Südhof, T. C. (1990) *Nature* **345**, 260–263
- Tsien, R. Y. (1998) *Annu. Rev. Biochem.* **67**, 509–544
- Chapman, E. R., and Jahn, R. (1994) *J. Biol. Chem.* **269**, 5735–5741
- Davletov, B. A., and Südhof, T. C. (1993) *J. Biol. Chem.* **268**, 26386–26390
- Fernandez, I., Arac, D., Ubach, J., Gerber, S. H., Shin, O., Gao, Y., Anderson, R. G., Südhof, T. C., and Rizo, J. (2001) *Neuron* **32**, 1057–1069
- Geppert, M., Goda, Y., Hammer, R. E., Li, C., Rosahl, T. W., Stevens, C. F., and Südhof, T. C. (1994) *Cell* **79**, 717–727
- Voets, T., Moser, T., Lund, P. E., Chow, R. H., Geppert, M., Südhof, T. C., and Neher, E. (2001) *Proc. Natl. Acad. Sci. U. S. A.* **98**, 11680–11685
- Yoshihara, M., and Littleton, J. T. (2002) *Neuron* **36**, 897–908
- Fernández-Chacón, R., Königstorfer, A., Gerber, S. H., Garcia, J., Matos, M. F., Stevens, C. F., Brose, N., Rizo, J., Rosenmund, C., and Südhof, T. C. (2001) *Nature* **410**, 41–49
- Sorensen, J. B., Fernández-Chacón, R., Südhof, T. C., and Neher, E. (2003) *J. Gen. Physiol.* **122**, 265–276
- Tokuoka, H., and Goda, Y. (2003) *Neuron* **38**, 521–524
- Fukuoka, M., Moreira, J. E., Lewis, F. M., Sugimori, M., Niinobe, M., Miko-shiba, K., and Llinas, R. (1995) *Proc. Natl. Acad. Sci. U. S. A.* **92**, 10708–10712
- Jorgensen, E. M., Hartwig, E., Schuske, K., Nonet, M. L., Jin, Y., and Horvitz, H. R. (1995) *Nature* **378**, 196–199
- Poskanzer, K. E., Marek, K. W., Sweeney, S. T., and Davis, G. W. (2003) *Nature* **426**, 559–563
- Zhang, J. Z., Davletov, B. A., Südhof, T. C., and Anderson, R. G. (1994) *Cell* **78**, 751–760
- Hauke, V., Wenk, M. R., Chapman, E. R., Farsad, K., and De Camilli, P. (2000) *EMBO J.* **19**, 6011–6019
- Han, W., Rhee, J. S., Maximov, A., Lao, Y., Mashimo, T., Rosenmund, C., and Südhof, T. C. (2004) *Neuron* **41**, 85–99
- Caroni, P. (1997) *J. Neurosci. Methods* **71**, 3–9
- Probst, A., Gotz, J., Wiederhold, K. H., Tolnay, M., Mistl, C., Jatou, A. L., Hong, M., Ishihara, T., Lee, V. M., Trojanowski, J. Q., Jakes, R., Crowther, R. A., Spillantini, M. G., Burki, K., and Goedert, M. (2000) *Acta Neuropathol.* **99**, 469–481
- Vidal, M., Morris, R., Grosveld, F., and Spanopoulou, E. (1990) *EMBO J.* **9**, 833–840
- Hogan, B., Constantini, F., and Lacey, E. (1994) in *Manipulating the Mouse Embryo: A Laboratory Manual* (Hogan, B., Constantini, F., and Lacey, E., eds) Cold Spring Harbor Laboratory Press, Cold Spring Harbor, NY
- Ashery, U., Betz, A., Xu, T., Brose, N., and Rettig, J. (1999) *Eur. J. Cell Biol.* **78**, 525–532
- Guan, K. L., and Dixon, J. E. (1991) *Anal. Biochem.* **192**, 262–267
- Sugita, S., Han, W., Butz, S., Liu, X., Fernández-Chacón, R., Lao, Y., and Südhof, T. C. (2001) *Neuron* **30**, 459–473
- Ubach, J., Lao, Y., Fernandez, I., Arac, D., Südhof, T. C., and Rizo, J. (2001) *Biochemistry* **40**, 5854–5860
- Shin, O. H., Rizo, J., and Südhof, T. C. (2002) *Nat. Neurosci.* **5**, 649–656
- Geppert, M., Ullrich, B., Green, D. G., Takei, K., Daniels, L., De Camilli, P., Südhof, T. C., and Hammer, R. E. (1994) *EMBO J.* **13**, 3720–3727
- Perin, M. S., Brose, N., Jahn, R., and Südhof, T. C. (1991) *J. Biol. Chem.* **266**, 623–629
- Lu, T., and Trussell, L. O. (2000) *Neuron* **26**, 683–694
- Hagler, D. J., Jr., and Goda, Y. (2001) *J. Neurophysiol.* **85**, 2324–2334
- Otsu, Y., Shahrezaei, V., Li, B., Raymond, L. A., Delaney, K. R., and Murphy, T. H. (2004) *J. Neurosci.* **24**, 420–433
- Schoch, S., Castillo, P. E., Jo, T., Mukherjee, K., Geppert, M., Wang, Y., Schmitz, F., Malenka, R. C., and Südhof, T. C. (2002) *Nature* **415**, 321–326
- Zucker, R. S., and Regehr, W. G. (2002) *Annu. Rev. Physiol.* **64**, 355–405
- Burke, N. V., Han, W., Li, D., Takimoto, K., Watkins, S. C., and Levitan, E. S. (1997) *Neuron* **19**, 1095–1102

<sup>2</sup> T. C. Südhof, unpublished observation.

42. Bennett, M. K., Calakos, N., and Scheller, R. H. (1992) *Science* **257**, 255–259
43. Li, C., Ullrich, B., Zhang, J. Z., Anderson, R. G., Brose, N., and Südhof, T. C. (1995) *Nature* **375**, 594–599
44. Chapman, E. R., Hanson, P. I., An, S., and Jahn, R. (1995) *J. Biol. Chem.* **270**, 23667–23671
45. Sollner, T., Bennett, M. K., Whiteheart, S. W., Scheller, R. H., and Rothman, J. E. (1993) *Cell* **75**, 409–418
46. Kee, Y., and Scheller, R. H. (1996) *J. Neurosci.* **16**, 1975–1981
47. Shin, O. H., Rhee, J. S., Tang, J., Sugita, S., Rosenmund, C., and Südhof, T. C. (2003) *Neuron* **37**, 99–108
48. Rickman, C., and Davletov, B. (2003) *J. Biol. Chem.* **278**, 5501–5504
49. Sugita, S., Hata, Y., and Südhof, T. C. (1996) *J. Biol. Chem.* **271**, 1262–1265
50. Chapman, E. R., An, S., Edwardson, J. M., and Jahn, R. (1996) *J. Biol. Chem.* **271**, 5844–5849
51. Damer, C. K., and Creutz, C. E. (1996) *J. Neurochem.* **67**, 1661–1668
52. Fernández-Chacón, R., Shin, O. H., Königstorfer, A., Matos, M. F., Meyer, A. C., Garcia, J., Gerber, S. H., Rizo, J., Südhof, T. C., and Rosenmund, C. (2002) *J. Neurosci.* **22**, 8438–8446
53. Wong, P. C., Cai, H., Borchelt, D. R., and Price, D. L. (2002) *Nat. Neurosci.* **5**, 633–639
54. Südhof, T. C. (2004) *Annu. Rev. Neurosci.* **27**, 509–547